



Article

# Acetabular Cups in 60 mm Metal-on-Metal Bearings Subjected to Dynamic Edge-Loading with 70° Peak-Inclination in 10-Million Cycle Simulator Study

Ian C. Clarke <sup>1,2,\*</sup>, Thomas Halim <sup>2</sup>, Evert J. Smith <sup>3</sup> and Thomas K. Donaldson <sup>4</sup><sup>1</sup> Department of Orthopedics, Loma Linda University Medical Center, Loma Linda, CA 92350, USA<sup>2</sup> DARF Retrieval Center, Colton, CA 92324, USA; Thomas.Halim@DARFcenter.org<sup>3</sup> Consultant Orthopedic Surgeon, Spire Hospital, Bristol BS6 6UT, UK; evert@evertsmith.com<sup>4</sup> Empire Orthopedics, 900 E Washington Blvd, Colton, CA 92324, USA; thomas.donaldson@gmail.com

\* Correspondence: Ian.Clarke@darfcenter.org; Tel.: +1-909-882-5867 (ext. x205)

Received: 25 October 2017; Accepted: 8 December 2017; Published: 21 December 2017

**Abstract:** Wear simulation of total-hip arthroplasty (THA) involves hip biomechanics, tribology, bearing designs and cup wear-patterns. This is the first demonstration of cup edge-loading using the “Inverted-cup” test mode. Benefits included, (i) clinically relevant wear-patterns, and (ii) cup inclinations varying from ideal to edge-loaded during each 1-s simulator cycle. The 60 mm head and cup bearings in metal-on-metal (MOM) hip joints showed run-in and steady-state wear phases to 10-million cycles (Mc). MOM edge-wear was not unduly high at 1.7 mm<sup>3</sup>/Mc overall, this 3-fold higher than 60 mm MOM study without edge-loading. One MOM outlier averaged 2.7 mm<sup>3</sup>/Mc, this representing the break-away wear (BAW) phenomena. A surprising result was that cups contributed 75–93% of total wear. The most disturbing conclusion from review of laboratory studies was that MOM wear-rates varied 1 to >30 mm<sup>3</sup>/Mc for reasons not understood. These data suggested a new hypothesis, that MOM bearings were very sensitive to external stimuli, be they simulator artifact or patient related.

**Keywords:** CoCr; hip-joint bearings; simulator; serum lubricant; 3rd-body wear

## 1. Introduction

Total hip arthroplasty (THA) is the definitive treatment for arthritis of the hip. It is the second most successful operation after cataract surgery and is performed in vast numbers throughout the world. Pioneering THA designs of the 1960–1970 era incorporated metal-on-polyethylene (MPE) and metal-on-metal (MOM) bearings, the latter using mainly cobalt-chrome alloys (as-cast CoCr). History shows that the 1st generation MOM bearings encountered many failures, considered multifactorial due to limited knowledge in design, instrumentation, and bone-fixation concepts [1–6]. In some cases, adverse CoCr wear produced severe biological reactions around the hip joints [3,7]. Nevertheless, subsequent studies showed some MOM patients achieved excellent clinical success, sometimes over 20 years [6,8–11].

In hip simulator laboratories, a major body of research identified fluid-film lubrication as one of the goals for achieving success with hip bearings [12–18]. Large MOM bearings appeared particularly suited to this concept. In the mid 1990’s, believing that problems with design, fixation and tribology had been addressed, implant companies developed the 2nd generation, large-diameter, MOM bearings. These included the femoral-head resurfacing type (Figure 1: RSA) and the now standard ball and socket configuration (Figures 2 and 3: THA). RSA and THA diameters ranged 36 to 60 mm and were widely accepted in their first ten years of use [19,20]. However, subsequent failures in many centers were blamed on production of CoCr debris and release of high concentrations of Co and Cr

ions [21–23]. Implant retrievals revealed that metal debris frequently blackened the hip capsules and surrounding musculature, the resulting production of pathological fluids, cysts, and tissue necrosis creating the appearance of “pseudotumors” [23–25]. This immune tissue response was termed an adverse reaction to metal debris (ARMD) [25]. Once again, cup design, surgical positioning and fixation were implicated as major risks for adverse wear. The most commonly reported failure mechanism appeared to be mechanical in origin, termed “edge loading” of steeply-inclined cups (Figure 1C) [21–23,26–31]. Edge-loading of THA bearings in patients’ hips may occur in several ways. For this report, we defined three likely mechanical risks as; (I) constant rim wear of the cup due to mal-positioned implants, (II) rim wear occurring intermittently at some extreme of patient motion, and (III) rim wear occurring intermittently due to hip-impingement episodes (head destabilized and forced over cup rim).

The second negative clinical experience with MOM bearings provided us with the incentive to re-examine methodology used in the simulator wear studies. Understanding and predicting performance of THA devices remains a complex and demanding task. Over a 5-decade history, hip-simulator laboratories developed pre-clinical wear tests that guided the medical industry [32–41]. Beginning in the 1960’s [42], wear-simulation of THA bearings contemplated integration of hip-joint biomechanics and tribology with many related parameters that included material combinations and implant designs. In addition, there were many patient variables to be considered (Figure 1), and much needed simplified to formulate feasible research protocols. Thus, simulator guidelines used by various regulatory agencies [43–45] represented a necessary simplification. The internationally accepted methodology shows the cup mounted above the femoral head (Figure 2), thereby simulating the “Anatomic” hip configuration as viewed on patient radiographs (Figure 1) [43]. The stipulated test inclination for the cup (Figure 2:  $60^\circ$  to load axis) represents a  $30^\circ$  angle ( $I^\circ$ ) in the simulator’s horizontal plane, this believed to approximate the  $45^\circ$  cup inclination in patients (Figure 1A).

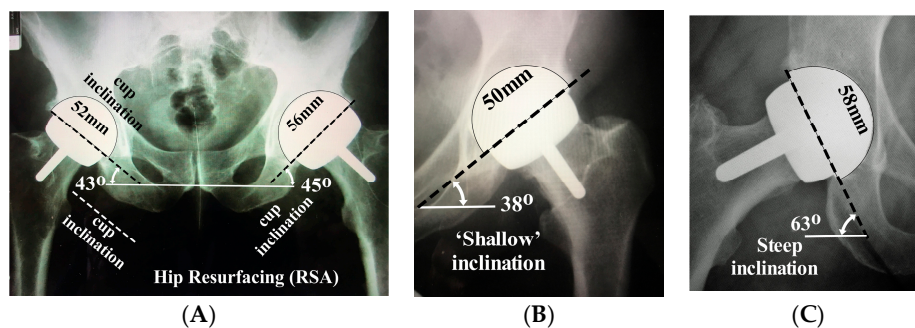


**Figure 1.** Radiographic images showing metal-on-metal (MOM) variations, (A) 52 and 56 mm diameters implanted at desired inclination  $43^\circ$ – $45^\circ$  (B) 50 mm cup at “shallow” inclination and (C) 58 mm cup at “steep” inclination.

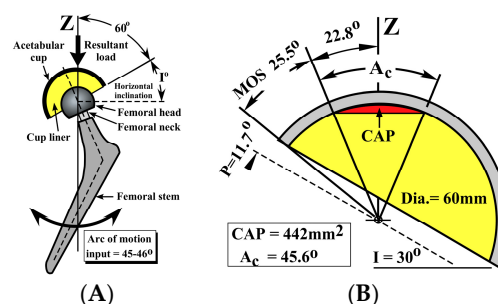


**Figure 2.** Guideline for “Anatomic-cup” test (ISO14241-1) [43], (A) hip implant loaded vertically (Z-axis) and (B) cup wear-pattern (CAP) in 60 mm diameter cup subtends angle ( $A$ ) =  $45.6^\circ$ . Large MOM cup has sub-hemispherical profile indicated by angle- $P$  =  $11.7^\circ$ . Mounted at test inclination ( $I$ ) =  $30^\circ$  this has large margin-of-safety ( $MOS$  =  $25.5^\circ$ ) before there is a risk for edge-loading at cup rim.



**Figure 3.** Size range of “large” MOM implants.

Wear studies with large-diameter MOM bearings followed standard simulator guidelines (Figure 2) with some preferring to use a 35° cup inclination [46–55]. Resulting wear-rates appeared acceptably low at 0.5 to 0.8 mm<sup>3</sup> per million load cycles (Mc). Three of these non edge-loaded studies also reported on their cup wear-patterns [46–48].

With emerging clinical insight regarding the risks of “edge-loading” in steeply inclined cups (Figure 1C) [21,30,31,49], simulator laboratories responded with steep-cup wear studies. All used the same simulator guideline, i.e., constant edge-loading of cup (fixed-inclination) that represented mode-I clinical risk. There were no guidelines for selection of test parameters. Cup inclinations were different in each study and MOM diameters varied 38.5 to 48 mm (Table 1). Even in non edge-loaded tests, it is recognized that some MOM bearings will produce much higher wear-rates for reasons unknown, i.e., “run-away wear” or “break-away wear” (“BAW”) trends [48,50,51]. Such BAW wear phenomenon represents a dramatic contrast to the anticipated classical run-in and steady-state wear phases (Table 2: “STD”). Thus, the large variation in steep-cup MOM wear-rates (1.9–19.5 mm<sup>3</sup>/Mc) remained open to interpretation (Table 1).

**Table 1.** Test parameters in simulator wear studies of “steep-cups”.

Study	Simulator Type	Implant Vendor	MOM Dia. (mm)	Cup Angle (I°)	Test Duration	Avg. Wear-Rate (mm <sup>3</sup> /Mc)
Kamali 2008 [52]	Prosim	S&N	50	* NS	3 Mc	* 1.5
Williams 2008 [53]	Leeds	Depuy	28	45	5 Mc	1.4
Leslie 2009 [54]	Prosim	Depuy	38.5	50	2 Mc	5.5
Angadji 2009 [55]	MTS	Corin	40	60	3.5–6 Mc	1.9
Hu 2011 [56]	Prosim	Finsbury	48	65	2 Mc	19.5

**Key:** Dia: MOM diameter, \* “steep cups” but not edge-loaded, NS: not specified, S&N: Smith & Nephew, I°: cup inclination. Mc: a million load-cycles.

**Table 2.** 60 mm Anatomic-cup data with six matched MOM bearings [48], four with classical run-in and steady-state wear phases (“STD”) and two bearings showing “breakaway wear” (“BAW”) phenomenon.

Parameters in 60 mm MOM Study [48]	STD	BAW	Ratio BAW/STD
Average MOM wear-rates (mm <sup>3</sup> /Mc)	0.6	1.6	2.7
Cup wear-area (CAP mm <sup>2</sup> )	442	745	1.7
60 mm hemispherical area (H mm <sup>2</sup> )	5655	5655	-
Cup-hemi-area ratio (CAP/H)	7.8%	13.2%	-
Head wear area (HAP mm <sup>2</sup> )	1668	1942	1.2
Head hemi-area ratio (HAP/H)	29.5%	34.3%	1.2
Wear-area ratios (HAP/CAP)	3.78	2.61	0.7
CAP-angle ( $A_c$ )	45.6	59.5	1.3
HAP-angle ( $A_h$ )	90.3	97.9	1.1

The severity of edge-loading will depend to what degree the normal wear-pattern becomes truncated by the cup rim. This can only be determined if size and location of wear patterns are known. In an earlier study, we developed an algorithm that predicted wear-pattern areas and the degree of edge-loading likely to be present in a patient’s MOM hip joint [57]. As a simulator test method (Figure 4), when the cup-profile angle ( $P$ ), and its included angle ( $A_c$ ) are known, the margin-of-safety (MOS) protecting the cup from edge-loading can be calculated using,

$$I + P + \text{MOS} + A_c/2 = 90^\circ \quad (1)$$

The rim angle ( $P$ ) for the sub-hemispherical profile of large diameter cup is given by,

$$2 \times P + \text{CF} = 180^\circ \quad (2)$$

The wear area (CAP = 442 mm<sup>2</sup>) measured in 60 mm cups [48] subtended a wear-pattern angle ( $A_c$ ) estimated (using standard spherical equations) to be 45.6°. The profile angle in this large, sub-hemispherical cup was given by  $P = 11.7^\circ$ . Therefore, the 45° test inclination used (Figure 4) would produce a margin-of-safety of MOS = 10.5° (Equation (1)), i.e., no edge-loading. This Anatomic-cup study [48] also revealed that measured head wear-areas averaged 3.78-fold greater than in cups (Table 2). This is a result of the head’s  $\pm 23^\circ$  orbit under the simulator’s load-axis (Z). The wear-pattern formed on the head (Figure 4) subtends the angle  $A_h = A_c + 46^\circ = 91.6^\circ$ . Using standard spherical equations, it can be shown that this larger wear-pattern has an estimated area of 1712 mm<sup>2</sup>, i.e., 3.87× times larger than in cups. This calculation validated our previous experimental wear-pattern ratio [48].

Notable in the prior Anatomic-cup study was that wear-patterns on heads represented 29% to 34% of the nominal surface area but cups only 7% to 13% (Table 2). As visualized on our large plastic models, head and cup wear-patterns presented dramatically different areas (Figure 5). It was therefore notable that implant retrieval studies with MOM and ceramic-on-metal (COM) bearings revealed that wear-patterns in vivo extended over 50–60% of nominal cup surfaces [58,59]. With a goal to creating clinically-relevant cup wear-patterns in edge-loading simulations, we decided that a novel test strategy would be to reverse the standard Anatomic-cup configuration. Simply mounting the cups in the inverted position would change the distributed wear-pattern from heads (Figure 5) to cups. This new strategy also introduced a constantly varying cup inclination, which would simulate for the first time the mode-II clinical risk of edge-loading [60].

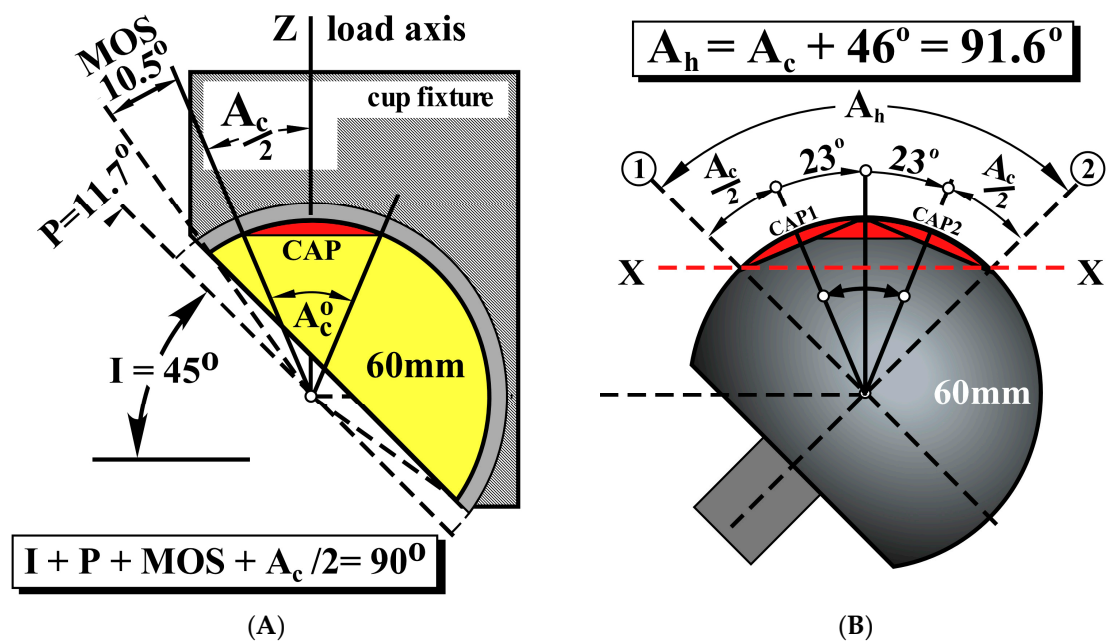


**Figure 4.** Illustration of “Anatomic-cup” configuration using a 60 mm bearing, (A) Cup wear-pattern CAP = 442 mm<sup>2</sup> area [48] subtends angle  $A_c = 45.6^\circ$ . With cup-profile angle  $P = 11.7^\circ$ , the algorithm predicts the estimated margin-of-safety’ is  $MOS = 11.7^\circ$ , and (B) as the head orbits a  $\pm 23^\circ$  arc under load-axis (Z), the head’s wear pattern will extend, as indicated by CAP1 and CAP2 areas. The resulting distributed wear-pattern on head (at level of plane X-X) will subtend angle  $A_h = A_c + 46^\circ = 91.6^\circ$ .

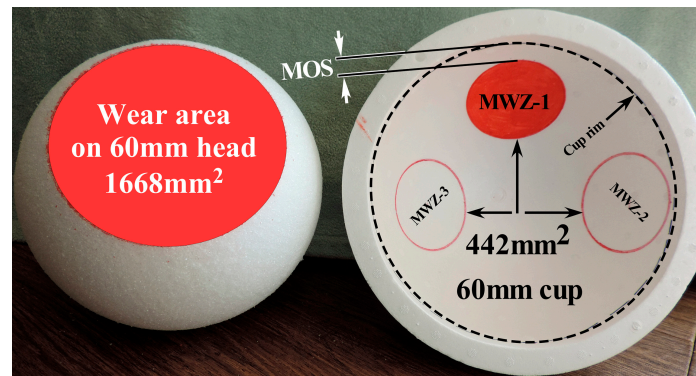


**Figure 5.** Wear patterns from 60 mm MOM study [48] scaled on plastic model to contrast magnitudes of wear-areas on heads and cups. Three cup wear-patterns are positioned to show the margin of safety (MOS) present at inclinations (1)  $50^\circ$ , (2)  $60^\circ$  and (3)  $35^\circ$ .

Our trial MOM simulator study with Inverted-cups (1 Mc duration) validated the algorithm’s predictions, showing no edge-loading evident with cup inclinations peaking at  $40^\circ$  and  $50^\circ$  (Figure 6A) [60]. The follow-up wear study with  $70^\circ$  peak cup inclination produced edge-loading over 5 Mc duration. Wear-pattern analysis showed edge wear was achieved and validated over 5 Mc duration (Figure 6B) [60].

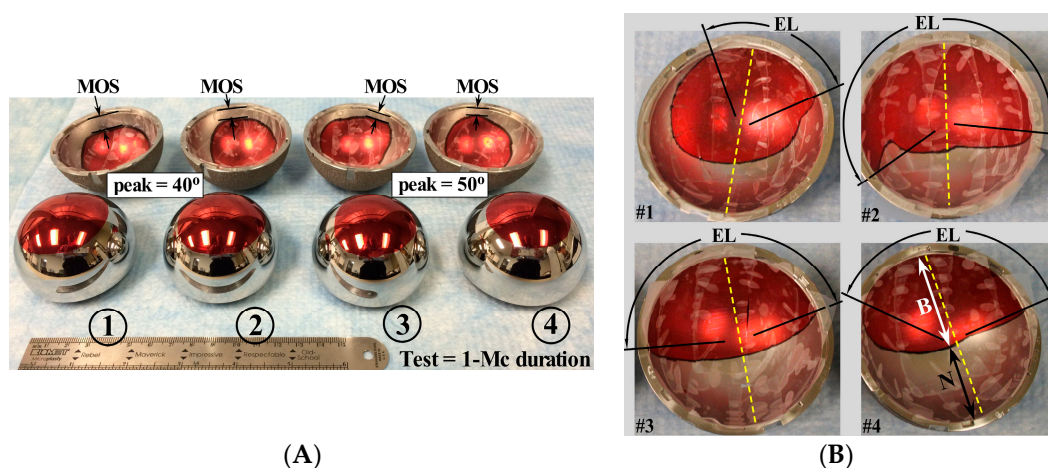


**Figure 6.** MOM wear-patterns stained red for photography to show margin-of-safety (MOS), non-worn areas (N) and arcs of rim wear representing edge-loading (EL): for (A) 1 Mc validation test (non edge-loaded) with margin-of-safety visible in four cups (inclination I-peak = 40°, 50°), and (B) 5 Mc wear test (edge-loaded) with four cups (inclination I-peak = 70°) showing large arcs of rim wear (EL).

Compared to the 60 mm Anatomic-cup test [48], edge-loading in Inverted-cups produced approximately 3-fold higher wear-rates (Table 3) [60]. This was an encouraging result but the 5 Mc wear study suffered from two limitations. Gravimetric wear assessment of the bearings was compromised due to transfer of proteinaceous debris from the lubricant [61,62]. This contamination appeared during “run-in” and “steady-state” wear phases. In addition, one test-station experienced a simulator-cam failure, resulting in initial loss of one MOM bearing. These limitations reduced the effectiveness of the Inverted-cup model and also made wear predictions uncertain for 60 mm MOM. Therefore, the purpose of the current study was to extend the Inverted-cup test from 5-million [60] to 10-million cycles. This longer duration would aid definition of steady-state wear and thereby provide better estimates for run-in wear-rates. The hypotheses were that, (1) wear trends in 60 mm heads and cups would be linear from 5 to 10-million cycles duration, (2) re-assessment of run-in wear phases would reveal transition to steady-state wear occurred prior to 0.75 Mc duration, (3) 60 mm MOM wear-rates would average 1.7 to 2 mm<sup>3</sup>/Mc overall [60], and (4) cup wear magnitude would represent >70% of total MOM wear [48].

**Table 3.** 60 mm MOM wear-rates compared in Anatomic [48] and Inverted [60] tests to 5 Mc.

Volumetric Wear-Rates (mm <sup>3</sup> /Mc)	Run-in Wear-Rate	Steady-State Wear-Rate	Overall Wear-Rate
60 mm Anatomic test [48]	1.6	0.4	0.7
60 mm Inverted test [60]	6.0	1.4	2.0
Wear ratios Inverted/Anatomic	3.8	3.1	2.9

## 2. Materials and Methods

The four 60 mm MOM bearings used in the 10-million cycle study were the originals donated for the 5 Mc study [60] by DJO-Global (Austin, TX, USA). The cups were mounted at a 47° face angle in Polyacetal adaptors (Figure 7A) with locking rings and anti-rotation pegs to guard against high torques associated with large CoCr bearings. The orbital hip simulator (Shore Western, Monrovia, CA, USA) was identical to that used in the prior study and test methods duplicated that work [60]. Bearing wear was assessed by gravimetric techniques at each 0.5 Mc interval.

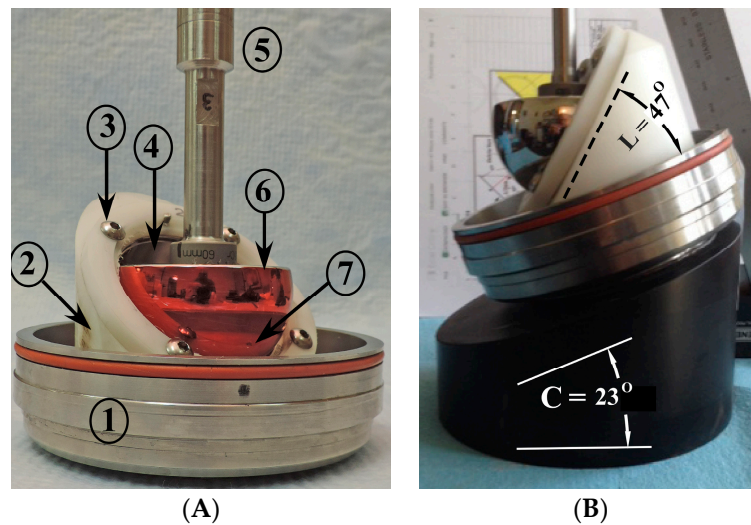


**Figure 7.** Test chamber configuration for Inverted-cups, (A) baseplate (1) has  $47^\circ$ -inclined adaptor (2) installed with locking ring and locking screws (3) to secure CoCr liner (4). Steel shaft (5) attaches femoral head (6) to load-cell in Z-axis. (B) Simulator cam orbiting  $\pm 23^\circ$  provides cup inclinations from  $23^\circ$  to  $70^\circ$  each second of the machine cycle. Head-exposure at  $70^\circ$  cup inclination is even more extreme than indicated at  $47^\circ$  home inclination in (A).

The Inverted-cup method provided variable edge-loading conditions. The four cups set with inclination  $L = 47^\circ$  in the home-cam position (Figure 7B) alternated between “shallow” ( $I = 24^\circ$ ) and “steep” ( $I = 70^\circ$ ) inclinations during each 1-s orbit of the simulator cam ( $C = \pm 23^\circ$ ). As in prior studies, the bovine-serum lubricant (Hyclone, Ogden, UT, USA) was diluted 30% to a concentration of 20 mg/mL in each 450 mL test chamber [48,60]. New lubricant was installed after each cleaning cycle. Weight-loss changes due to wear were measured at 0.5-million cycle intervals to 10 Mc duration. Implant cleaning procedures were rigorous in anticipation of protein contamination from lubricant precipitation. When weight-gain trends were identified, those bearings were taken back for inspection and additional cleaning. Head and cup weight-loss trends were compared by linear-regression techniques and box-plot analyses from 1 to 10 Mc duration. In the 5 Mc Inverted-cup study, MOM-1 was omitted from consideration [60] and remaining three MOM bearings used for analysis. The present study continued in this way but re-introduced MOM-1 for comparison. Bearing wear areas were identified visually and by light microscopy, stained red for photography and taped to minimize cup reflections (Figure 6) [48,60].

In prior studies without edge-loading (Figure 6A), it was possible to track the size of head and cup wear-patterns (CAP  $\text{mm}^2$ ;  $A^\circ$ ) and the margin of safety (MOS $^\circ$ ). In the prior Anatomic-cup study, wear-patterns on heads averaged  $1668 \text{ mm}^2$  in area [48]. The trial Inverted study (1 Mc,  $17^\circ$  inclination) produced virtually identical cup wear-patterns (average area  $1663 \text{ mm}^2$ ) [60]. Using standard equations for spherical geometry, the corresponding control angle ( $A^\circ$ ) for cup wear-patterns in this study was calculated as  $A = 90.2^\circ$ . The corresponding measured MOS-angles  $15.4^\circ$  and  $5.3^\circ$  for  $17^\circ$  and  $27^\circ$ -mounted cups demonstrated the  $10^\circ$  shift in wear-patterns [60].

In contrast, an edge-loading test has no margin-of-safety and the standard wear-pattern ( $A^\circ$ ) will be truncated by the cup rim. For this test, we tracked estimated non-wear ( $N^\circ$ ) and truncated wear-zone ( $B^\circ$ ) angles predicated on simulator cam-rotation being  $\pm 23^\circ$  (Table 4). At the cam’s home position (Figure 8), the truncated wear-pattern was estimated as  $B = 82.4^\circ$ , this representing  $7.8^\circ$  of edge-loading. As the cam rotates down to its minimum position, cup inclination will reduce to  $24^\circ$  thereby providing a  $15.2^\circ$  margin-of-safety. As the cam rotates up to maximum position, cup inclination increases to  $70^\circ$  thereby indicating  $E = 30.8^\circ$  as the maximum edge-loading.

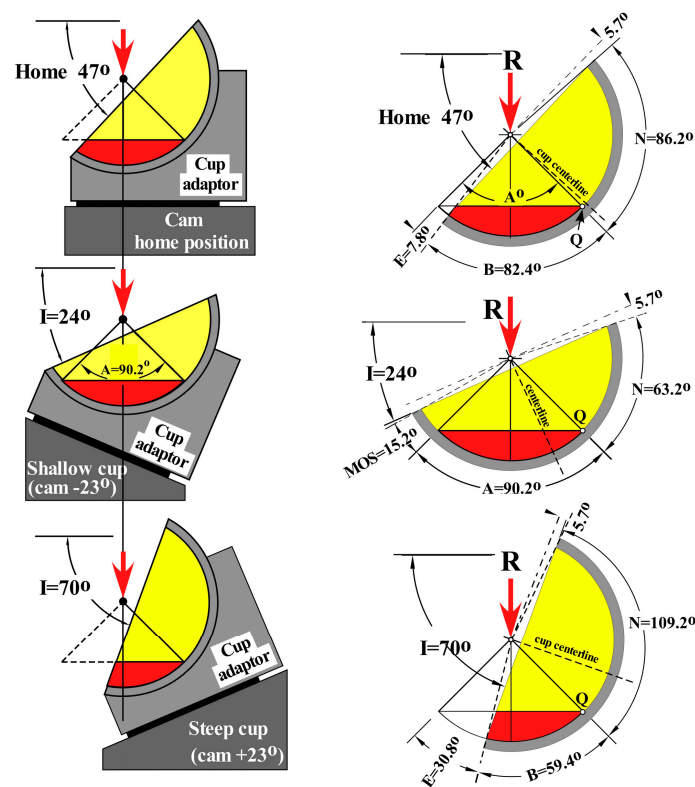


**Figure 8.** Schematic cross-section of 60 mm cup showing wear-pattern ( $A = 90.2^\circ$ ) centered on simulator load axis: (A) at home-position of cam ( $C = 0$ ), cup inclination is  $I = 47^\circ$  with edge-loading indicated by  $E = 7.8^\circ$ , (B) at minimum position ( $C = -23^\circ$ ), cup inclination is  $I = 24^\circ$  with margin-of-safety indicated by  $MOS = 15.2^\circ$  and (C) at maximum position ( $C = +23^\circ$ ), cup inclination is  $I = 70^\circ$  and edge-loading is indicated by  $E = 30.8^\circ$ .  $A_c$ : angle subtended by cup wear area (non-edge loaded),  $B$ : angle subtended by truncated wear-pattern (edge-loaded),  $E$ : edge-wear angle,  $MOS$ : margin-of-safety,  $N$ : angle subtended by non-wear zone, and  $R$ : vertical axis for simulator loading.

**Table 4.** Angular geometry estimated for 60 mm wear-patterns (cup home-position angle,  $L = 47^\circ$ ).

Tracking Inverted-Cup Parameters	Low-Cam	Home	High-Cam
Wear-pattern area ( $A^\circ$ )	90.2	90.2	90.2
Home-mount inclination ( $L^\circ$ )	47	47	47
Cam angle ( $C^\circ$ )	-23	0	23
Cup inclination ( $I^\circ$ )	24	47	70
Cup profile ( $P^\circ$ )	5.7	5.7	5.7
Cup margin of safety ( $MOS^\circ, E^\circ$ )	15.2	-7.8	-30.8
Edge loading (EL%)	none	-9%	-34%
Truncated wear pattern ( $B^\circ$ )	none	82.4	59.4
Non-wear zone ( $N^\circ$ )	63.2	86.2	109.2

With non-wear angle ( $N^\circ$ ) estimated to vary  $63^\circ$  to  $109^\circ$  (Table 4), the home position (Figure 8: datum Q) was used as a control to track measurements comparing the estimated values  $N = 86.2^\circ$  and  $B = 82.4^\circ$ . At 8.5, 9.5 and 10 Mc durations, the corresponding of B-chords and N-chords of cup wear-patterns (Figure 5) were measured and converted to angular data for analysis.

It was necessary to predict the degree of edge-loading represented in each wear study. Here the critical inclination ( $I_c$ ) is defined as that cup position where  $MOS = \text{zero}$ , i.e., cup wear = pattern is juxtaposed to the cup rim, and given by

$$I_c + P + A_c/2 = 90^\circ \quad (3)$$

The severity of edge-loading (EL) may be defined as,

$$EL = (I_c - I)/I \quad (4)$$

For the 60 mm cup in Anatomic test mode, the critical inclination was calculated as  $I_c = 61.5^\circ$  (Table 5). In the Inverted test, the larger wear-pattern lowers the critical cup inclination to  $I_c = 39.1^\circ$ . Estimated risks of edge-wear were, (i) 9% edge-loading at home-cam position, (ii) 34% edge-loading at high-cam position, these contrasting with (iii) margin-of-safety MOS =  $15.2^\circ$  at the low-cam position (Figure 8).

**Table 5.** Comparison of Anatomic [48] and Inverted-cup [60] data.

Test Parameters	Anatomic	Inverted	Ratio
MOM diameter (mm)	60	60	
Cup wear area (mm <sup>2</sup> )	442	1672	3.87
60 mm hemispherical area (mm <sup>2</sup> )	5655	5655	
Cup hemi-area ratio	7.6%	29.6%	3.89
Critical inclination angle (°)	61.5	39.1	63%

For comparison of published “steep-cup” data (Table 1) it was necessary to determine the wear-pattern (A) and profile (P) angles applicable to each cup design. It is known that the initial contact areas enlarge as bearing wear progresses during run-in phase [46–48]. When the contact-stresses are sufficiently reduced to allow optimal tribological conditions, the resulting equilibrium producing lower wear-rates in the “steady-state” phase. The steady-state wear-patterns measured in MOM studies with no edge-loading typically ranged 380 to 480 mm<sup>2</sup> in area (Table 6). These averaged approximately 4-fold larger than contact-areas predicted using Hertzian equations for elastic deformation of spheres (Figure 9A). The wear-pattern angles ( $A_c$ ) were calculated (using standard spherical equations) for large diameter cups (38–60 mm) and plotted (Figure 9B). This treatment revealed a linear relationship, with angle- $A_c$  inversely proportional to cup diameter (D mm). Omitting two outliers (#1, 8), the wear-pattern angle ( $A_c$ ) was defined by,

$$A = 99.697 - 0.9099 \times D \quad (5)$$

**Table 6.** Cup wear-areas converted to wear-pattern angles ( $A_c$ ), this table ranked by diameter.

ID#	STUDY	Simulator	Vendor	Dia (mm)	DC (mm)	CAP (mm <sup>2</sup> )	$A_c$
1	Leslie 2008 [46]	Prosim-2	Depuy	38.5	0.111	429	70.7
2	Lee 2008 [47]	MTS-orbital	Stryker	40	0.15	383	64.1
3	Lee 2008 [47]	MTS-orbital	Stryker	40	0.4	364	62.4
4	Leslie 2008 [46]	Prosim-2	Depuy	54.5	0.126	474	52.1
5	Lee 2008 [47]	MTS-orbital	Stryker	56	0.15	416	47.4
6	Lee 2008 [47]	MTS-orbital	Stryker	56	0.4	419	47.6
7	Bowsher 2009 [48]	SWM-orbital	Comis	60	0.24	442	45.6
8	Bowsher 2009 [48]	** SWM-orbital	Comis	60	0.24	745	59.5

KEY = Dia: cup diameter, DC: diametral clearance (cup-head), CAP: cup wear-pattern,  $A_c$ : angle subtended by wear-pattern.

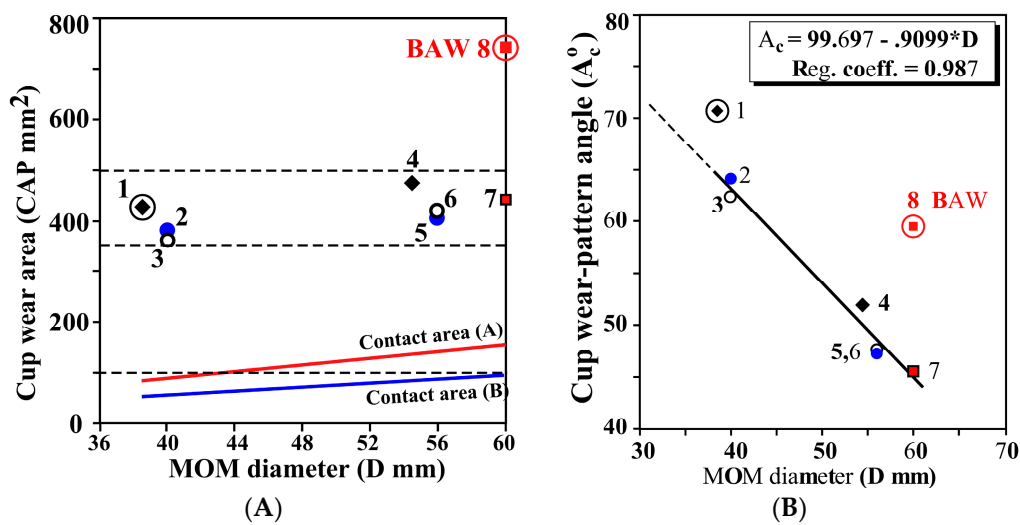


**Figure 9.** Wear areas (CAP) in non edge-loaded cups as identified in Table 6 [46–48], (A) comparison of Hertzian contact-areas with cup wear-patterns (parameters: CoCr modulus = 220 GPA, Poisson’s ratio = 2.9, diametral clearance,  $A = 0.1$  mm and  $B = 0.2$  mm), and (B) linear regression analysis for wear-pattern angles ( $A_c$ ) plotted with respect to diameter. Data #1 and #8 were omitted as outliers, datum #8 reflecting the break-away wear (BAW) phenomenon [48].

### 3. Results

As plotted over 10-million cycles duration (Figure 10), it was apparent overall that, (i) heads and cups demonstrated run-in wear and both showed steady-state wear phases 1 to 10 Mc duration, (ii) cups (#2–4) produced more wear than heads (#1–4), and (iii) total wear in cup-1 was approximately double that of the other cups. Cup wear-patterns stained for photography at 10 Mc duration demonstrated the truncated (B) and large non-wear areas (N) typical of edge-loaded cups (Figure 11). Their area assessments were represented on average by angles  $N = 86.3^\circ$  and  $B = 82.5^\circ$ .

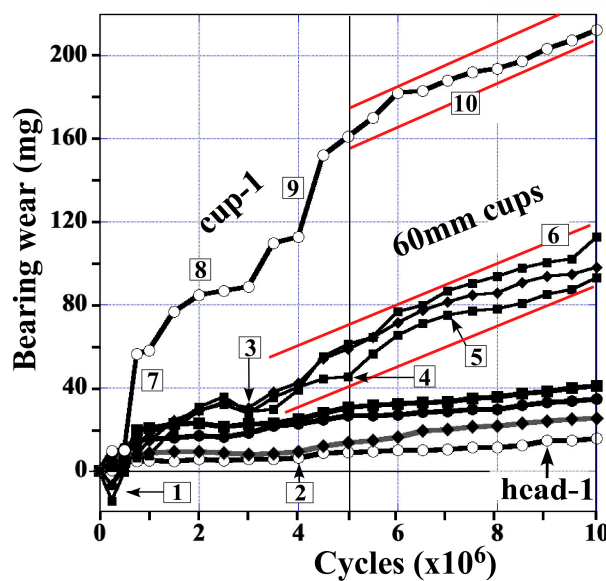


**Figure 10.** Head and cup wear data over 10 Mc test.

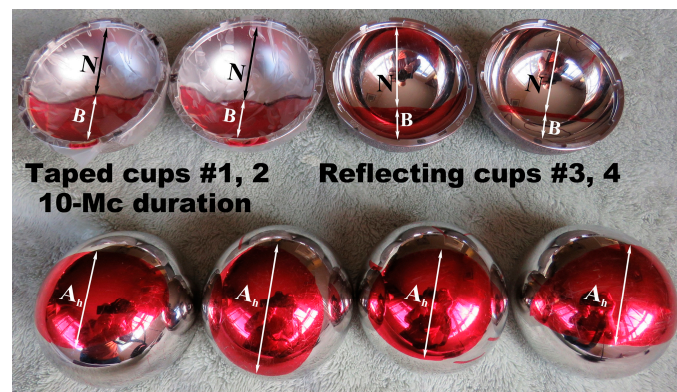


**Figure 11.** Wear patterns marked on 60 mm bearings at 10 Mc duration, showing cups #1, 2 taped, and cups #3, 4 reflecting their mirror-like bearing surfaces, measurements included wear-patterns ( $A_h$ ) on heads (arrows), truncated wear-patterns ( $B$ ) and non-wear ( $N$ ) areas in cups.

All cups showed an initial weight-gain artifact due to adherence of protein contaminants (Figure 10: Flag-1). Cups #2–4 behaved similarly as a group, revealing a 2nd weight-gain artifact at 3 Mc (Flag-3). Their wear trends appeared to plateau at 5 Mc (Flag-4) and again at 8 Mc (Flag-5). Even with cyclical weight-gain artifacts evident, the overall wear in cups trended linearly to provide an average wear-rate of  $9.9 \text{ mg/Mc} \pm 10\%$  over 1 to 10 Mc (Figure 12A: minimum  $R = 0.98$ ). Extrapolating steady-state trends back to the Y-axis, revealed cups #2–4 transitioned into steady-state phase by 1.5 Mc (Figure 12B). Omitting the weight-gain artifacts at 0.25 Mc, cup run-in wear-rates were estimated to be 13.4 to 16.3 mg/Mc, averaging 14.9 mg/Mc. This run-in estimation was 1.5-times greater than their ensuing steady-state trend. Cup-1 in this study showed anomalous behavior. By 1 Mc it produced a run-in wear magnitude of 58 mg (Figure 10: Flag-7). By 2 Mc duration, it appeared to be transitioning into a steady-state phase (Flag-8) only to accelerate with another run-in wear phase to 5 Mc (Flag-9). The final steady-state wear phase 5 to 10 Mc appeared reasonably linear (Flag-10)  $9.2 \text{ mg/Mc}$  and a good match to that of cups #2–4 (Flag-6).

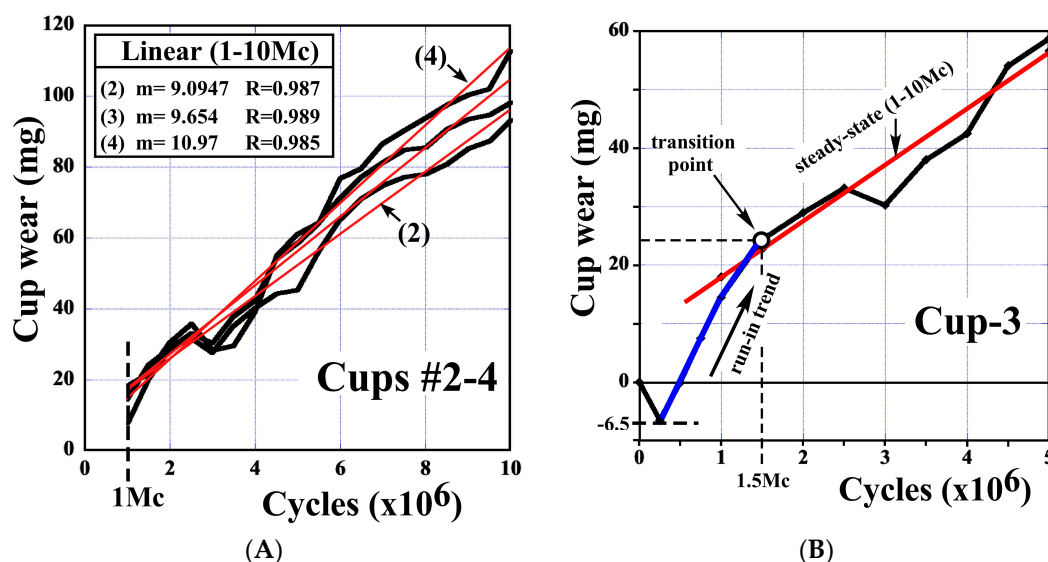


**Figure 12.** Wear trends in cups #2–4, (A) 1–10 Mc duration and (B) transition of cup-3 at 1.5 Mc intersection with its steady-state trend.

Heads #1–4 did not show any weight-gain artifacts as measured initially in cups. Their steady-state wear trending was negligible to 4 Mc (Figure 10: Flag-4) and they only began to demonstrate some mild

wear beyond 5 Mc. It was interesting that head-1 with the lowest wear-rate was paired with the highest wearing cup-1. Regression analysis for steady-state wear in heads #1–4 averaged 2.3 mg/Mc ± 5% (Figure 13A: 1–10 Mc), indicating good precision with high regression coefficients (minimum R = 0.96). Extrapolating steady-state trends back to the Y-axis revealed heads transitioned into steady-state phase by 0.75 Mc (Figure 13B). These data provided run-in wear estimates ranging 7 to 20 mg/Mc, with average 19.1 mg/Mc. This run-in wear estimation for heads was 8.3-times greater than the ensuing steady-state trend.

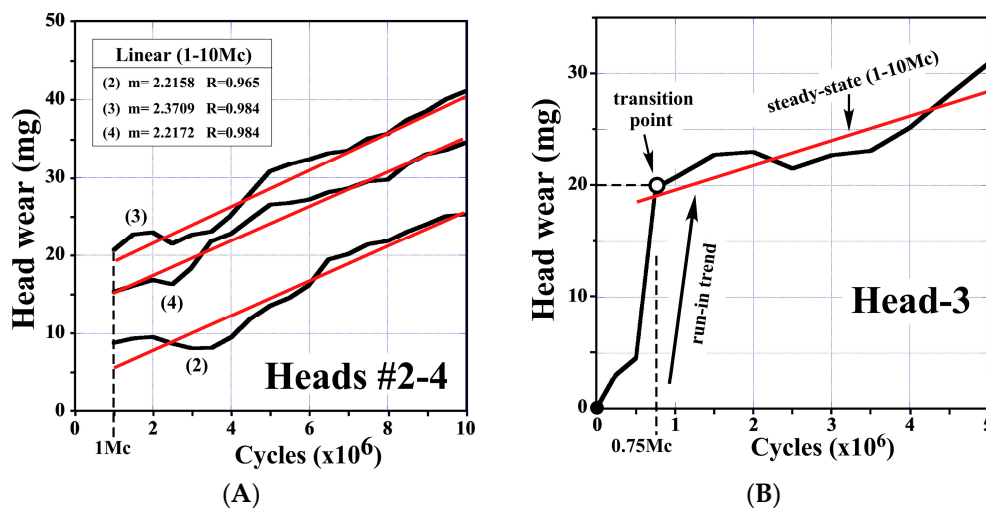


Figure 13. Wear trends in heads #2–4, for (A) 1–10 Mc duration and (B) transition of head-3 at 0.75 Mc intersection with its steady-state trend.

At 10 Mc duration, the cumulative volume of wear in three MOM bearings (#2–4) represented 17.1 mm<sup>3</sup> with cup wear providing 75% of total (Figure 14). The corresponding wear volume in MOM-1 was 27.9 mm<sup>3</sup> (Figure 12), with cup wear providing 93% of total.

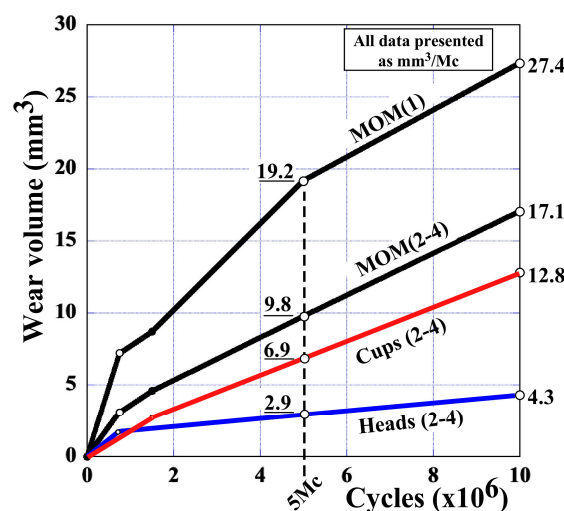


Figure 14. Volumetric wear for heads, cups, and combined totals (MOM) over 10 Mc test duration.

#### 4. Discussion

This simulator study examined the wear response of 60 mm metal-on-metal (MOM) bearings run to 10-million cycles duration (10 Mc) with cups mounted under transient edge-loading conditions. This may be the first simulator study using an algorithm to predict severity of edge-loading in

steeply-inclined cups. The 60 mm cup diameter represented the largest in wear studies to date and featured the largest margin of safety (MOS). The standard Anatomic-cup test, defined in international simulator guidelines, was reversed in this study so that hip motion could be input via the acetabular cup. This created the larger cup wear-patterns considered more clinically-relevant for simulation of edge-loading. This novel method also provided the first demonstration of intermittent edge-loading in steeply-inclined cups (mode-II clinical risk) rather than the standard fixed edge-loading condition (mode-I clinical risk). With cup inclination varying continuously ( $24^\circ$  to  $70^\circ$ ) in each cycle period of 1-s, the overall wear-rate in three MOM bearings averaged  $1.7 \text{ mm}^3$  per million cycles while one MOM, considered an outlier, was almost 60% higher at  $2.7 \text{ mm}^3$  per million cycles. The Inverted-cup model demonstrated satisfactory run-in and steady-state wear phases to 10 Mc duration in both heads and cups, thereby satisfying hypothesis #1.

There are three major considerations in laboratory wear simulations, namely (1) experimental design, (2) credibility of wear trends, and (3) clinical relevance. The most disturbing result from this review of both standard and steep-cup MOM wear studies was that laboratory wear-rates varied from less than 1 to over  $19 \text{ mm}^3/\text{Mc}$  for reasons not understood and with no guidelines available for selection of test parameters (Table 1). In particular, the severity of edge-loading will depend to what degree the normal wear-pattern becomes truncated by the cup rim. This can only be determined if size and location of wear-patterns are known. In an earlier clinical study, we used an algorithm to predict wear-patterns and severity of cup edge-loading in MOM patients [57]. This was extended to our 60 mm MOM simulator study to validate size and location of wear-patterns. The trial study with Inverted-cups used two tests with cyclic cup-inclinations  $-6^\circ$  to  $40^\circ$  and  $4^\circ$  to  $50^\circ$  to verify “non edge-loaded” conditions and one with  $24^\circ$  to  $70^\circ$  inclination to verify “edge-loading” status [60]. The present 10 Mc wear study satisfactorily demonstrated edge-loading, the resulting MOM wear-rates averaging  $1.7 \text{ mm}^3/\text{Mc}$ . Applying these new estimates back to the 5 Mc-datum provided overall wear-rate  $2 \text{ mm}^3/\text{Mc}$ . This was approximately 3-fold greater wear than our Anatomic study with non edge-loaded cups [48]. These results served to validate the experimental design of the Inverted-cup test, and also confirmed our 3rd hypothesis.

It is well documented that protein contamination from serum lubricants can be a confounding problem in gravimetric wear assessments [61–64]. Our prior 5 Mc study revealed major contamination confounded the wear assessments [60]. This was partly anticipated because we reported a similar cyclic phenomenon in 28 mm MOM studies [63,64]. We extended the 60 mm MOM study from 5 Mc to 10 Mc to provide more credibility to wear predictions in the Inverted-cup method. Possibly because 60 mm bearings were capable of greater frictional torque, there may have been a more conspicuous deposition of proteins that were well bonded onto CoCr surfaces (Figure 15). However, even with this limitation, linear regression trends taken over 9-million cycles proved sufficiently robust for steady-state wear assessments. By extension backwards to the Y-axis, new estimates were determinable for head and cup run-in trends. This showed that best-fit for run-in wear transitioning into steady-state was at 0.75 Mc and 1.5 Mc for heads and cups, respectively. Therefore, hypothesis #2 stating that heads and cups would transition into steady-state phase before 1 Mc was not fully satisfied. Comparing 10 Mc to 5 Mc data (Table 4), it was apparent that the short-duration test had underestimated run-in wear-rates for heads and overestimated that for cups (Table 7). However, the largest discrepancy in the prior 5 Mc study was underestimating steady-state wear-rates in heads. The new data revealed that heads had higher run-in wear-rates but for a shorter duration than cups. As a result, both transitioned into their steady-state phases after approximately the same amount of wear was produced during run-in (Figures 12B and 13B).

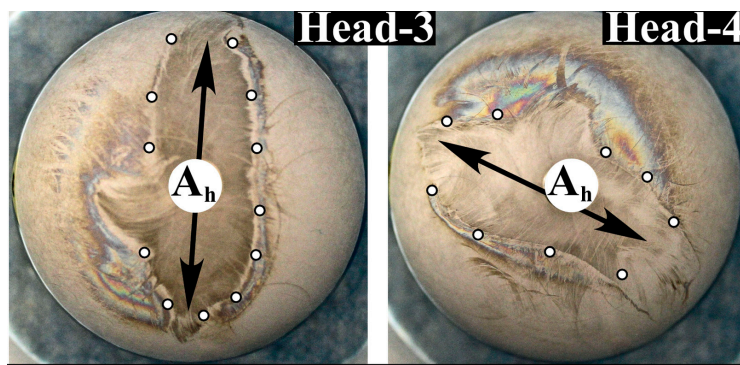


**Figure 15.** Photographs of iridescent-appearing protein contaminants well bonded to femoral heads after 250,000 cycles in 10 Mc wear test. Protein outlines (dotted) approximately correspond to boundary ( $A_h$ ) of head wear-patterns indicated in Figure 11.

**Table 7.** Comparison of wear-rates in Inverted-cup tests (mg/Mc) at 5 Mc and 10 Mc.

Wear-Rate Trends	5 Mc	10 Mc	Ratio 10 Mc/5 Mc
Heads run-in	14.3	19.1	135%
Cups run in	35.3	14.9	42%
Heads steady-state	0.9	2.3	252%
Cups steady-state	10.5	9.9	94%

A major confounding effect in MOM simulator studies has been the appearance of unexplained, usually high wear-rates that appeared transiently for 1 to 3 Mc duration. Such wear phenomena, variously described as “runaway” or “break-away” (“BAW”) wear, appeared in non edge-loaded tests, and were estimated to occur in 15% to 40% of MOM bearings [48,50,51]. A 50 mm MOM study [50] demonstrated one of five bearings produced 3-times higher wear by 3 Mc with subsequent recovery over 2 Mc duration (Figure 16A). A similar 40 mm MOM study noted adverse wear in three of eight bearings (38%), cup wear-rates being noted in excess of 30 mm<sup>3</sup>/Mc [51]. It was noted that one of three cups demonstrated a recovery by 2.5 Mc duration, producing minimal steady-state wear thereafter (Figure 16B). This BAW phenomenon presented as a major confounding event, particularly when the typical simulator study has only small numbers of replicates, i.e.,  $N = 2$  to 8 bearings.

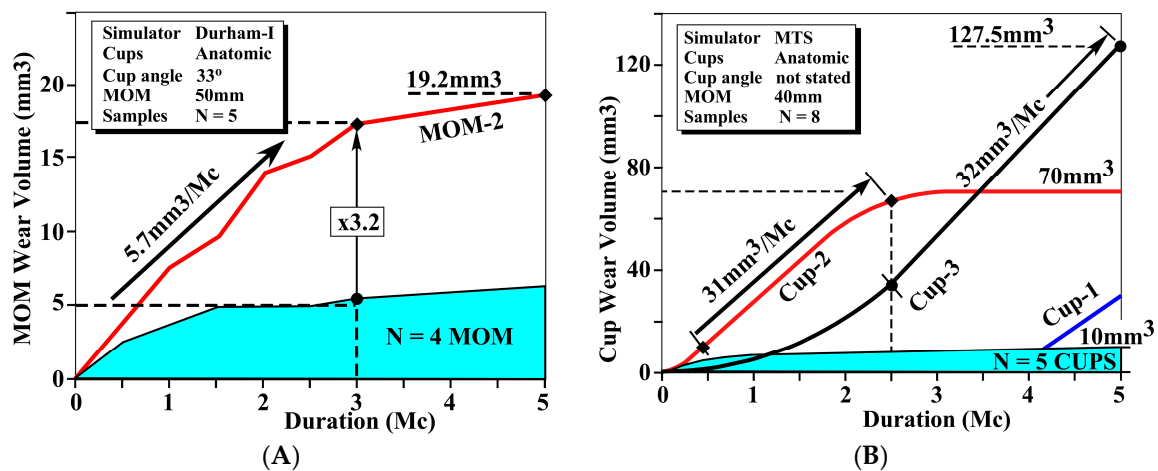


**Figure 16.** Anomalous wear behavior depicted in Anatomic-cup studies (non edge-loaded), (A) one in five of 50 mm MOM (BHR, Smith and Nephew) [50] and (B) three in eight of 40 mm MOM (Stryker) [51].

In the present study, MOM-1 bearing produced an overall wear-rate of  $2.7 \text{ mm}^3/\text{Mc}$ , approximately 60% greater than the other bearings (Figure 14). Our laboratory noted that the station-1 cam-bearings were replaced early in the 5 Mc study, apparently indicating a problem that could have triggered adverse wear. However, with hindsight, we would now ascribe MOM-1's trend to an extended "BAW run-in" phase to 5 Mc duration (Figure 10), similar to those previously described (Figure 16). It was also notable that the break-away wear-rates (BAW) described in the prior 60 mm Anatomic study [48] were of similar magnitude, averaging  $2.1 \text{ mm}^3/\text{Mc}$  overall. However, these wear-rates were quite modest compared to data in some MOM studies (Table 8). A surprising result was in the degree of wear experienced by 60 mm cups. At 5 Mc in the prior Anatomic study, wear in BAW-cups represented 85% of total, compared to 68% in standard cups (STD). At 5 Mc in the Inverted study, the corresponding cup wear ratios were BAW = 95% and STD = 70%, these satisfying hypothesis 4. Prior steep-cup studies did not provide individual head and cup wear-rates [53,55], so there were no other comparisons at 5 Mc duration. Given these examples of MOM wear variations, we are of the opinion that such "MOM outliers" should be included as part of the overall assessment.

**Table 8.** High transient wear-rates in appearing in MOM studies.

Study	Vendor	Diameter (mm)	Inclination ( $I^\circ$ )	Duration (Mc)	MOM Wear-Rate ( $\text{mm}^3/\text{Mc}$ )
* Bowsher 2009 [48]	Comis	60	45	1.5	* 2.1
Present study	DJO	60	24–70	5	2.7 <sup>+</sup>
+ Leslie 2009 [54]	Depuy	38.5	50	2	5.5 <sup>+</sup>
Vassiliou 2006 [50]	S&N	50	33	3	5.7
+ Hu 2011 [56]	Finsbury	48	65	2	19.7 <sup>+</sup>
** Essner 2005 [51]	Stryker	40	NS	2.5	** 31.7

\* Bowsher: Break-away wear (BAW), \*\* Essner: cup wear-rate only, <sup>+</sup>: edge-loading study.

The clinical relevance of laboratory wear tests is quite difficult to assess. A hip simulator study represents a complex undertaking while still representing an over-simplification of patient conditions. A major body of work over the years identified fluid-film lubrication as the ideal condition for success in MOM bearings [12,13,16]. However, MOM bearings failing in patients have demonstrated adverse wear mechanisms that can produce significantly high volumes of CoCr debris within a few years [21–23]. The radiographic presentation of steeply-inclined cups has frequently been criticized, many studies citing "edge loading" as major evidence for adverse MOM wear in patients [21,22,24,27,29–31,49]. It is therefore interesting that three very different simulator studies of edge-loaded cups [53,55,60] produced MOM wear-rates elevated compared to control data (Table 1) but still within the range ( $0.5$  to  $2 \text{ mm}^3/\text{Mc}$ ) considered typical of many MOM simulator studies [65]. In prior 3rd-body wear studies with CoCr and Ti6Al4V particulates, wear-rates  $> 3 \text{ mm}^3/\text{Mc}$  turned the MOM lubricants black [66]. This was not experienced in this 10 Mc study of edge-loaded bearings.

This 10 Mc study is the first Inverted-cup model with test inclinations varying each cycle, simulating a patient achieving edge-loading only intermittently during the activities of daily living (mode-II clinical risk). Our suspicion was that the Inverted-cup model might produce less wear than steep-cup studies running with full-time edge-loading (mode-II clinical risk). A 40 mm Anatomic-cup study run to 6 Mc duration appeared the most comparable data [55]. The  $1.9 \text{ mm}^3/\text{Mc}$  wear-rate in 40 mm cups inclined  $60^\circ$  appeared almost identical to our 60 mm Inverted-cup study with  $2 \text{ mm}^3/\text{Mc}$  overall wear-rate (Figure 14: 5 Mc duration) However, the question was how comparable were two tests using different MOM designs, very different cup diameters and differing test inclinations? The MOM algorithm predicts that the wear-pattern angle in a 40 mm cup would be  $A_c = 63.3^\circ$  (Equation (5)). The cup-face angle (CF) for a 40 mm Cormet cup (Corin Group PLC, Cirencester, UK) was published elsewhere as  $159^\circ$  [31]. Equation (2) provides the cup-profile angle as  $P = 10.5^\circ$  and from Equation (3), the critical cup inclination was estimated as  $I_c = 48^\circ$ . Therefore, the  $35^\circ$ ,  $50^\circ$  and  $60^\circ$  fixed-cup inclinations would have test conditions given by, (i)  $MOS = 13^\circ$ , (ii)  $E = 2^\circ$  and

(iii)  $E = 12^\circ$ , respectively. The latter two angles represented edge-loading condition of  $EL = 3\%$  and  $19\%$  (Equation (4)). Edge-loading conditions in our Inverted-cup study varied from  $MOS = 15^\circ$  to  $EL = 9\%$  and peaked at  $EL = 34\%$  in each duty cycle (Table 4). While such similarities in two studies are intriguing, they remain purely speculative until more simulator data is accumulated. However, these two simulator studies with full-time and intermittent edge-loading conditions did not produce the much-cited adverse wear blamed on steeply-inclined cups. In fact, both showed the typical run-in and steady-state wear typical of stable MOM wear trends. This suggested that the appearance of adverse wear mechanisms may be triggered by additional circumstances.

Hip impingement in particular represents an unavoidable and we believe a major clinical risk for production of large 3rd-body metal particulates. As illustrated (Figure 17), when the femoral implant of either CoCr or Ti6Al4V alloy can impact against the acetabular cup, the CoCr liner rim (Figure 17: #1) may notch the neck (Figure 17: #2), releasing either CoCr or Ti6Al4V particles [58,67,68]. The resulting destabilization of the hip-joint allows large hip muscles to force head rotation (or migration #3) over the cup rim (#4) during such episodes, creating large linear scratches on heads (#5) [58] and releasing large quantities of 3rd-body CoCr particles [58,69]. Frequent head subluxations may also produce gross erosion of the liner rim (#4 [48]). We termed this phenomenon “repetitive sub-clinical subluxation” (RSS) because our patients were generally unaware of it [70]. It is both unpredictable and of unknown severity and consequences. Therefore we hypothesize that patient activities may result in hip micro-separation and impingement episodes that release large CoCr particles into the joint space [58,68]. We know that introduction of metallic particles greatly accelerates wear of MOM bearings, consistently turning simulator lubricants black in color at wear-rates greater than  $3 \text{ mm}^3/\text{Mc}$  [66]. With ensuing activities of daily living, we further propose that the resulting 3rd-body wear mechanisms produce adverse wear until the CoCr particles are either worn small enough over time to escape or become ionized [58]. However, continuing hip-impingement episodes will initiate further release of metal particulates.

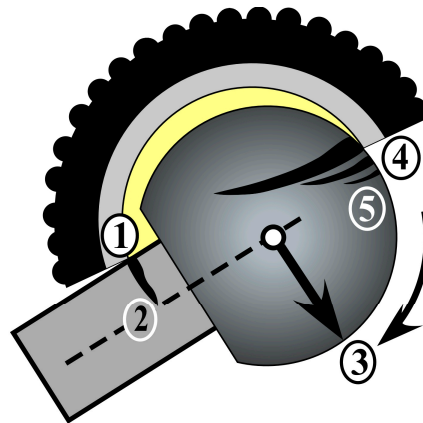


**Figure 17.** Illustrating effects of CoCr liner in the acetabular cup impinging against the femoral neck during various patient activities (redrawn from Clarke and Manley, 2008) [68].

In summary, the most disturbing result from this review of both standard and steep-cup wear studies is that MOM wear-rates in laboratory studies have varied widely for reasons not well understood. Even with purposefully matched bearings studied in expert laboratories, MOM wear performance has proved unpredictable and quite erratic [48,50,51,54,56]. Thus, the large range of MOM wear measured in laboratory studies may in itself be a warning that the risk of adverse wear conditions in MOM patients is very high. These combined observations suggest a new hypothesis, that MOM bearings are extremely sensitive to external influences, be they simulator artifacts, or patient related.

## 5. Conclusions

1. This MOM simulator study incorporating the Inverted-cup concept demonstrated two clinically-relevant benefits, (i) cup-inclinations that varied during each 1-s simulator cycle and (ii) large cup wear-patterns that approached the clinical norm.
2. The large margin of safety (MOS) inherent in 60 mm MOM bearings was eliminated using a 70° peak cup-inclination. Arcs of rim-wear were evident in four cups run to 10-million cycles (10 Mc), validating predictions of the edge-loading algorithm.
3. Three 60 mm MOM completed their run-in wear phases by 1.5 Mc and thereafter demonstrated steady-state wear. The 10 Mc wear-rate averaged 1.7 mm<sup>3</sup>/Mc overall for these edge-loaded cups, averaging 3-fold greater than prior study without edge-loading.
4. One MOM bearing extended its run-in phase to approximately 4 Mc in a “break-away wear” (BAW) phenomenon, then demonstrated steady-state wear to 10 Mc. This BAW trend represented 2.7 mm<sup>3</sup>/Mc overall.
5. For comparisons to other 5 Mc studies, overall wear-rates for Inverted-cups averaged approximately 2 mm<sup>3</sup>/Mc in three bearings and increased to 3.8 mm<sup>3</sup>/Mc in one with a BAW-trend to 5 Mc duration. Given the history of MOM tribology and the many negative clinical reports, it would appear necessary to consider all such wear trends. In this study, the four MOM bearings averaged 2.4 mm<sup>3</sup>/Mc over 5 Mc duration but did not meet our 3 mm<sup>3</sup>/Mc simulator criterion representing adverse MOM wear producing black-colored lubricants.
6. The most disturbing result from this review of both standard and steep-cup studies was that MOM simulator wear-rates varied from 1 to 30 mm<sup>3</sup>/Mc for reasons not understood. This in itself warns that the risk of adverse results with MOM bearings is very high.

**Acknowledgments:** The simulator study to 5-million cycles was supported by an FDA contract titled “Development and Validation of Improved Premarket Testing methods for Metal-on-Metal (MOM) Hip Replacements” (FDA-1090372). The MOM study 5 to 10-million cycles was supported by the Arthroplasty for Arthritis Foundation (UK charity# 1051165) and the DARF Center, Colton, CA, USA. We thank M. Burgett, P. Williams, and R. Moran for their technical assistance and the DJO Group (Austin, TX, USA) for donation of 60 mm MOM implants.

**Author Contributions:** Thomas K. Donaldson and Evert J. Smith provided MOM expertise and implant retrieval information that defined the scope of the simulator project. Experimental goals were formulated by Ian C. Clarke, Thomas K. Donaldson and Evert J. Smith. Thomas Halim and Ian C. Clarke performed the simulator experiments and analyzed the wear data. Ian C. Clarke wrote the paper with medical input and manuscript reviews contributed by Thomas K. Donaldson and Evert J. Smith (See Appendix A).

**Conflicts of Interest:** The authors declare no conflicts of interest.

## Appendix A

### Evert Smith

Consultant Orthopaedic Surgeon

Evert J Smith (EJS) is a Consultant Orthopaedic Surgeon undertaking private practice in London and Bristol UK (Spire Hospital Bristol, Nuffield Bristol Hospital, The Lister Hospital, London). From 1996 until July 2017 he practiced for the National Health Service (NHS) at North Bristol NHS Trust and was Honorary Consultant Senior Clinical Lecturer for the University of Bristol at this time. His clinical and surgical experience is revision and primary hip surgery, complex primary and revision surgery and he has implanted and revised a significant number of metal on metal (MoM) hip devices, both resurfacing arthroplasty and total hip arthroplasty (THA).

EJS developed an interest in biomechanics and bearing surfaces of the hip during his Fellowship at Harvard University in the Orthopaedic Department of Massachusetts General Hospital and he was design/developer of the Exceed and Exceed ABT systems (Biomet UK).

He is a founder member of the Orthopaedic Data Evaluation Panel UK where analysis of survival outcomes of hip implants according to National Institute for Health and Care Excellence guidelines

is undertaken (2002 to the present); and a member of the Beyond Compliance group which has been established to regulate and manage strict market entry criteria for hip implants following the high failure rate of MoM implants. From its inception in 2003 to December 2016 EJS was Regional Co-ordinator for the South West of England for the National Joint Registry for England, Wales, Northern Ireland and the Isle of Man (NJR), and Bearings Surface Evaluator. He is the British Hip Society representative for the European Hip Society (EHS) as well as being a member of the EHS Scientific Committee where he is involved in the organisation, management of the EHS international annual congress. EJS has organised and coordinated the international annual Bristol Hip Arthroplasty Course (BHAC) from 2003 to the present, and he regularly lectures at international conferences in his area of expertise. As well as being a well published author, he is peer reviewer for high impact orthopaedic journals and Associate Editor in Chief UK for Reconstructive Review Journal (USA).

EJS is founder and Director of the Arthroplasty for Arthritis Charity (A4A), a charitable resource which undertakes research into current technologies and surgical practice in joint replacement, targeted at both improving the performance of implants and the survival outcomes of implants <http://www.a4ach.org/site/uk/arthroplasty-for-arthritis>. DARF has been the recipient of two research grants from A4A, one in 2014 and another in 2016.

A research collaboration was formed between EJS, Professor Ian Clarke (ICC) and Thomas K Donaldson (TKD) of the Donaldson Arthritis Research Foundation (DARF) in 2006. ICC and TKD have both participated as faculty at several BHAC meetings since 2007 and EJS joined the faculty for the 10th Hip & Knee Arthroplasty and Bearing Surfaces Conference in California in 2008. This affiliation resulted in EJS, Alun John Orthopaedic Surgeon Cardiff and Vale University Health Board NHS and ICC soliciting the FDA for MoM contracts. The first successful application was number FDA1090360 in 2011 and three further FDA contracts were won in 2012. The resultant research has produced ground-breaking knowledge, and a great deal of information has been published. This information has been instrumental in regulating the use of, and monitoring of patients with MoM technologies, as well as producing valuable information for the orthopaedic community which will bring about improved outcomes for patients.

## References

1. Wilson, J.N.; Scales, J.T. The Stanmore metal on metal total hip prosthesis using a three pin type cup. A follow-up of 100 arthroplasties over nine years. *Clin. Orthop. Relat. Res.* **1973**, *95*, 239–249. [[CrossRef](#)]
2. McKee, G.K.; Chen, S.C. The statistics of the McKee-Farrar method of total hip replacement. *Clin. Orthop. Relat. Res.* **1973**, *95*, 26–33. [[CrossRef](#)]
3. Jones, A.D.; Lucas, H.K.; O'Driscoll, M.; Price, C.H.G.; Wibberley, B. Cobalt Toxicity after McKee Hip Arthroplasty. *J. Bone Jt. Surg. Br.* **1975**, *57*, 289–296.
4. Murray, M.P.; Gore, D.R.; Brewer, B.J.; Zuege, R.C.; Gardner, G.M. Comparison of functional performance after McKee-Farrar, Charnley, and Muller total hip replacement. A six-month follow-up of one hundred sixty-five cases. *Clin. Orthop. Relat. Res.* **1976**, *121*, 33–43.
5. Tillberg, B. Total hip arthroplasty using the McKee & Watson-Farrar prosthesis. *Acta Orthop. Scand.* **1982**, *53*, 103–107. [[PubMed](#)]
6. August, A.C.; Aldam, C.H.; Pynsent, P.B. The McKee-Farrar hip arthroplasty. A long-term study. *J. Bone Jt. Surg. Br.* **1986**, *68*, 520–527.
7. Coleman, R.F.; Herrington, J.; Scales, J.T. Concentration of wear products in hair, blood, and urine after total hip replacement. *Br. Med. J.* **1973**, *1*, 527–529. [[CrossRef](#)] [[PubMed](#)]
8. McKellop, H.; Park, S.H.; Chiesa, R.; Doorn, P.; Lu, B.; Normand, P.; Grigoris, P.; Amstutz, H. *In Vivo Wear of 3 Types of Metal on Metal Hip Prostheses during 2 Decades of Use*; Clinical Orthopaedics and Related Research: Atlanta, GA, USA, 1996; Volume 329, pp. 128–140.
9. Schmalzried, T.P.; Szuszczewicz, E.S.; Akizuki, K.H.; Petersen, T.D.; Amstutz, H.C. Factors correlating with long term survival of McKee-Farrar total hip prostheses. *Clin. Orthop. Relat. Res.* **1996**, *329*, S48–S59. [[CrossRef](#)]

10. Weber, B.G. Metasul from 1988 to today. In *Metasul A Metal-on-Metal Bearing*; Rieker, C., Windler, M., Wyss, U., Eds.; Hans Huber: Bern, Switzerland, 1999; pp. 23–28.
11. Campbell, P.; Urban, R.M.; Catelas, I.; Skipor, A.K.; Schmalzried, T.P. Autopsy analysis thirty years after metal-on-metal total hip replacement. A case report. *J. Bone Jt. Surg. Am.* **2003**, *85*, 2218–2222. [[CrossRef](#)]
12. Goldsmith, A.A.; Dowson, D.; Isaac, G.H.; Lancaster, J.G. A comparative joint simulator study of the wear of metal-on-metal and alternative material combinations in hip replacements. *Proc. Inst. Mech. Eng.* **2000**, *214*, 39–47. [[CrossRef](#)] [[PubMed](#)]
13. Dowson, D.; McNie, C.M.; Goldsmith, A.A.J. Direct experimental evidence of lubrication in a metal-on-metal total hip replacement tested in a joint simulator. *Proc. Inst. Mech. Eng. Part C-J. Mech. Eng. Sci.* **2000**, *214*, 75–86. [[CrossRef](#)]
14. Scholes, S.C.; Unsworth, A. The tribology of metal-on-metal total hip replacements. *Proc. Inst. Mech. Eng.* **2006**, *220*, 183–194. [[CrossRef](#)] [[PubMed](#)]
15. Brockett, C.; Harper, P.; Williams, S.; Isaac, G.; Dwyer-Joyce, R.; Jin, Z.; Fisher, J. Direct measurement of lubrication in large diameter metal-on-metal hip implants. In Proceedings of the 53rd Annual Meeting of the Orthopaedic Research Society, San Diego, CA, USA, 11–14 February 2007; Volume 32, p. 1653.
16. Isaac, G.H.; Siebel, T.; Schmalzried, T.P.; Cobb, A.G.; O’Sullivan, T.; Oakeshott, R.D.; Flett, M.; Vail, T.P. Development rationale for an articular surface replacement: A science-based evolution. *Proc. Inst. Mech. Eng.* **2006**, *220*, 253–268. [[CrossRef](#)] [[PubMed](#)]
17. Isaac, G.H.; Thompson, J.; Williams, S.; Fisher, J. Metal-on-metal bearings surfaces: Materials, manufacture, design, optimization, and alternatives. *Proc. Inst. Mech. Eng.* **2006**, *220*, 119–133. [[CrossRef](#)] [[PubMed](#)]
18. Liu, F.; Leslie, I.; Williams, S.; Fisher, J.; Jin, Z. Development of computational wear simulation of metal-on-metal hip resurfacing replacements. *J. Biomech.* **2008**, *41*, 686–694. [[CrossRef](#)] [[PubMed](#)]
19. McMinn, D.; Treacy, R.; Lin, K.; Pynsent, P. Metal on metal surface replacement of the hip. Experience of the McMinn prosthesis. *Clin. Orthop. Relat. Res.* **1996**, *329*, S89–S98. [[CrossRef](#)]
20. Amstutz, H.C.; Campbell, P.; McKellop, H.; Schmalzried, T.P.; Gillespie, W.J.; Howie, D.; Jacobs, J.; Medley, J.; Merritt, K. Metal on metal total hip replacement workshop consensus document. *Clin. Orthop. Relat. Res.* **1996**, *329*, S297–S303. [[CrossRef](#)]
21. Langton, D.; Jameson, S.; Joyce, T.; Hallab, N.; Natsu, S.; Nargol, A. Early failure of metal-on-metal bearings in hip resurfacing and large-diameter total hip replacement. A consequence of excess wear. *J. Bone Jt. Surg. Br.* **2010**, *92*, 38–46. [[CrossRef](#)] [[PubMed](#)]
22. Morlock, M.M.; Bishop, N.E.; Zustin, J.; Hahn, M.; Ruther, W.; Amling, M. Modes of Implant Failure After Hip Resurfacing: Morphological and Wear Analysis of 267 Retrieval Specimens. *J. Bone Jt. Surg. Am.* **2008**, *90*, 89–95. [[CrossRef](#)] [[PubMed](#)]
23. Pandit, H.; Glyn-Jones, S.; McLardy-Smith, P.; Gundle, R.; Whitwell, D.; Gibbons, C.L.M.; Ostlere, S.; Athanasou, N.; Gill, H.S.; Murray, D.W. Pseudotumours associated with metal-on-metal hip resurfacings. *J. Bone Jt. Surg. Br.* **2008**, *90*, 847–851. [[CrossRef](#)] [[PubMed](#)]
24. Kwon, Y.M.; Glyn-Jones, S.; Simpson, D.J.; Kamali, A.; McLardy-Smith, P.; Gill, H.S.; Murray, D.W. Analysis of wear of retrieved metal-on-metal hip resurfacing implants revised due to pseudotumours. *J. Bone Jt. Surg. Br.* **2010**, *92*, 356–361. [[CrossRef](#)] [[PubMed](#)]
25. Campbell, P.; Ebrazadeh, E.; Nelson, S.; Takamura, K.; De Smet, K.; Amstutz, H.C. Histological features of pseudotumor-like tissues from metal-on-metal hips. *Clin. Orthop. Relat. Res.* **2010**, *468*, 2321–2327. [[CrossRef](#)] [[PubMed](#)]
26. McLardy-Smith, P.; Steffen, R.T.; Pandit, H.; Murray, D.W.; Gill, H.S. Metal-on-metal hip resurfacing: America, where are you? *Orthopedics* **2006**, *29*, 795–796. [[PubMed](#)]
27. Langton, D.J.; Jameson, S.S.; Joyce, T.J.; Webb, J.; Nargol, A.V. The effect of component size and orientation on the concentrations of metal ions after resurfacing arthroplasty of the hip. *J. Bone Jt. Surg. Br.* **2008**, *90*, 1143–1151. [[CrossRef](#)] [[PubMed](#)]
28. Hart, A.J.; Hester, T.; Sinclair, K.; Powell, J.J.; Goodship, A.E.; Pele, L.; Fersht, N.L.; Skinner, J. The association between metal ions from hip resurfacing and reduced T-cell counts. *J. Bone Jt. Surg. Br.* **2006**, *88*, 449–454. [[CrossRef](#)] [[PubMed](#)]
29. Jameson, S.; Langton, D.; Nargol, A. Articular surface replacement of the hip: A prospective single-surgeon series. *J. Bone Jt. Surg. Br.* **2010**, *92*, 28–37. [[CrossRef](#)] [[PubMed](#)]

30. Kwon, Y.M.; Mellon, S.J.; Monk, P.; Murray, D.W.; Gill, H.S. In vivo evaluation of edge-loading in metal-on-metal hip resurfacing patients with pseudotumours. *Bone Jt. Res.* **2012**, *1*, 42–49. [[CrossRef](#)] [[PubMed](#)]
31. Underwood, R.J.; Zografos, A.; Sayles, R.S.; Hart, A.; Cann, P. Edge loading in metal-on-metal hips: Low clearance is a new risk factor. *Proc. Inst. Mech. Eng. H* **2012**, *226*, 217–226. [[CrossRef](#)] [[PubMed](#)]
32. Wright, K.W.J.; Scales, J. Stanmore Hip Joint Simulators for Study of Total Hip Joint Replacements. In *Evaluation of Artificial Joints*; Dowson, D., Wright, D., Eds.; The Biological Engineering Society, 1977; pp. 9–17.
33. Clarke, I.C. Wear of artificial joint materials IV. Hip joint simulator studies. *J. Eng. Med.* **1981**, *10*, 189–198. [[CrossRef](#)]
34. Streicher, R.M.; Semlitsch, M.; Schon, R.; Weber, H.; Rieker, C. Metal-on-metal articulation for artificial hip joints: Laboratory study and clinical results. *Proc. Inst. Mech. Eng. Part H J. Eng. Med.* **1996**, *210*, 223–232. [[CrossRef](#)] [[PubMed](#)]
35. Fisher, J.; Dowson, D. Tribology of total artificial joints. *Proc. Inst. Mech. Eng. H* **1991**, *205*, 73–79. [[CrossRef](#)] [[PubMed](#)]
36. Muratoglu, O.K.; Rubash, H.E.; Bragdon, C.R.; Burroughs, B.R.; Huang, A.; Harris, W.H. Simulated normal gait wear testing of a highly cross-linked polyethylene tibial insert. *J. Arthroplast.* **2007**, *3*, 435–444. [[CrossRef](#)] [[PubMed](#)]
37. Wang, A.; Stark, C.; Dumbleton, J.H. Mechanistic and morphological origins of ultra-high molecular weight polyethylene wear debris in total joint replacement prostheses. *Proc. Inst. Mech. Eng.* **1996**, *3*, 141–155. [[CrossRef](#)] [[PubMed](#)]
38. Semlitsch, M.; Streicher, R.M.; Weber, H. The wear behavior of capsules and heads of CoCrMo casts in long-term implanted all-metal hip prostheses. *Orthopade* **1989**, *5*, 377–381.
39. Affatato, S.; Terzi, S.; Nardi, D.; Toni, A.; Cianci, R. Metal-UHWMPE (Ultra High Molecular Weight Polyethylene) wear: Experimental testing. *Chir. Org. Mov.* **1997**, *82*, 393–399.
40. Ueno, M.; Amino, H.; Oonishi, H.; Clarke, I.C.; Good, V. *Wear of Alumina on Alumina Total Hip Prosthesis—Effect of Lubricant on Hip Simulator Test*; Bioceramics Giannini, S., Moroni, A., Eds.; Trans Tech Publications Ltd.: Zurich-Uetikon, Switzerland, 2000; pp. 561–564.
41. McKellop, H.A.; Campbell, P.; Park, S.H.; Schmalzried, T.P.; Grigoris, P.; Amstutz, H.C.; Sarmiento, A. The origin of submicron polyethylene wear debris in total hip arthroplasty. *Clin. Orthop. Relat. Res.* **1995**, *311*, 3–20.
42. Duff-Barclay, I.; Scales, J.T.; Wilson, J.N. Biomechanics. The development of the Stanmore total hip replacement. *Proc. R. Soc. Med.* **1966**, *59*, 948–951. [[PubMed](#)]
43. ISO. *14242-1: Implants for Surgery—Wear of Total Hip-Joint Prostheses—Part 1: Loading and Displacement Parameters for Wear-Testing Machines and Corresponding Environmental Conditions for Test*; ISO: Geneva, Switzerland, 2002.
44. ISO. *14242-2: Implants for Surgery—Wear of Total Hip-Joint Prostheses—Part 2: Methods of Measurement*; ISO: Geneva, Switzerland, 2000.
45. ISO. *14242-3: Implants for Surgery—Wear of Total Hip Joint Prostheses—Part 3: Loading and Displacement Parameters for Orbital Bearing Type Wear Testing Machines and Corresponding Environmental Conditions for Test*; ISO: Geneva, Switzerland, 2008.
46. Leslie, I.; Williams, S.; Brown, C.; Isaac, G.; Jin, Z.; Ingham, E.; Fisher, J. Effect of bearing size on the long-term wear, wear debris, and ion levels of large diameter metal-on-metal hip replacements—An in vitro study. *J. Biomed. Mater. Res. B Appl. Biomater.* **2008**, *87*, 163–172. [[CrossRef](#)] [[PubMed](#)]
47. Lee, R.; Essner, A.; Wang, A. Tribological considerations in primary and revision metal-on-metal arthroplasty. *J. Bone Jt. Surg. Am.* **2008**, *90*, 118–124. [[CrossRef](#)] [[PubMed](#)]
48. Bowsher, J.G.; Clarke, I.C.; Williams, P.A.; Donaldson, T.K. What is a “normal” wear pattern for metal-on-metal hip bearings? *J. Biomed. Mater. Res. B Appl. Biomater.* **2009**, *91*, 297–308. [[CrossRef](#)] [[PubMed](#)]
49. Mellon, S.J.; Kwon, Y.M.; Glyn-Jones, S.; Murray, D.W.; Gill, H.S. The effect of motion patterns on edge-loading of metal-on-metal hip resurfacing. *Med. Eng. Phys.* **2011**, *33*, 1212–1220. [[CrossRef](#)] [[PubMed](#)]
50. Vassiliou, K.; Elfick, A.P.; Scholes, S.C.; Unsworth, A. The effect of ‘running-in’ on the tribology and surface morphology of metal-on-metal Birmingham hip resurfacing device in simulator studies. *Proc. Inst. Mech. Eng. H* **2006**, *220*, 269–277. [[CrossRef](#)] [[PubMed](#)]

51. Essner, A.; Sutton, K.; Wang, A. Hip simulator wear comparison of metal-on-metal, ceramic-on-ceramic and crosslinked UHMWPE bearings. *Wear* **2005**, *259*, 992–995. [[CrossRef](#)]
52. Kamali, A.; Hussain, A.; Li, C.; Ashton, R.; Band, T. The Effect of Cup Orientation on the Tribological Performance of 50mm Birmingham Hip Resurfacing (BHR) Devices in a Hip Joint Wear Simulator. In Proceedings of the 54th Annual Meeting of the ORS, San Francisco, CA, USA, 2–5 March 2008.
53. Williams, S.; Leslie, I.; Isaac, G.; Jin, Z.; Ingham, E.; Fisher, J. Tribology and wear of metal-on-metal hip prostheses: Influence of cup angle and head position. *J. Bone Jt. Surg. Am.* **2008**, *90*, 111–117. [[CrossRef](#)] [[PubMed](#)]
54. Leslie, I.J.; Williams, S.; Isaac, G.; Ingham, E.; Fisher, J. High cup angle and microseparation increase the wear of hip surface replacements. *Clin. Orthop. Relat. Res.* **2009**, *467*, 2259–2265. [[CrossRef](#)] [[PubMed](#)]
55. Angadji, A.; Royle, M.; Collins, S.N.; Shelton, J.C. Influence of cup orientation on the wear performance of metal-on-metal hip replacements. *Proc. Inst. Mech. Eng. H* **2009**, *223*, 449–457. [[CrossRef](#)] [[PubMed](#)]
56. Hu, X.; Jeffers, J.; Roques, A.; Taylor, A.; Tuke, M. In vitro wear study of MOM and COM Hip Prostheses with High Cup Angle. In Proceedings of the ORS Annual Meeting, Long Beach, CA, USA, 13–15 January 2011.
57. Clarke, I.C.; Lazennec, J.Y. Margin-of-safety Algorithm used with EOS imaging to Interpret MHRA Warning for Small-diameter MOM Hip Arthroplasty. *Reconstr. Rev.* **2015**, *5*, 13–21. [[CrossRef](#)]
58. Clarke, I.C.; Donaldson, T.K.; Burgett, M.D.; Smith, E.J.; Bowsher, J.; Savisaar, C.; John, A.; Lazennec, J.Y.; McPherson, E.; Peters, C.L. Normal and adverse wear patterns created in-vivo on MOM surfaces—A retrieval study representing four vendors. In *Metal-on-Metal Total Hip Replacement Devices*; Kurtz, S.M., Greenwald, S.A., Mihalko, W.M., Lemons, J.A., Eds.; ASTM International: West Conshohocken, PA, USA, 2013; pp. 157–192.
59. Koper, M.C.; Mathijssen, N.M.C.; Claasen, H.H.R.; Witt, F.; Morlock, M.M.; Vehmeijer, S.B.W. Pseudotumor after bilateral ceramic-on-metal total hip arthroplasty. *J. Bone Jt. Surg. JBIS Case Connect.* **2014**, *4*, e25. [[CrossRef](#)]
60. Clarke, I.C.; Shelton, J.C.; Bowsher, J.; Savisaar, C.; Donaldson, T. Simulator Model Demonstrating Intermittent Edge-loading of Steeply-inclined MOM Bearings—A Clinically-relevant Incorporation of Cup-flexion Motion. *Reconstr. Rev.* **2017**, *7*. [[CrossRef](#)]
61. Maskiewicz, V.K.; Williams, P.A.; Prates, S.J.; Bowsher, J.G.; Clarke, I.C. Characterization of protein degradation in serum-based lubricants during simulation wear testing of metal-on-metal hip prostheses. *J. Biomed. Mater. Res. B Appl. Biomater.* **2010**, *91*, 429–440.
62. Burgett, M.D.; Donaldson, T.K.; Clarke, I.C. Denatured Protein Deposits Identical on Simulator and Explanted Hip Bearings. In *ASTM Symposium on Metal-on-Metal Total Hip Replacement Devices*; Kurtz, S.M., Greenwald, S.A., Mihalko, W.M., Lemons, J.A., Eds.; ASTM International: West Conshohocken, PA, USA, 2013; pp. 310–322.
63. Anissian, H.L.; Stark, A.; Gustafson, A.; Good, V.; Clarke, I.C. Metal-on-metal bearing in hip prosthesis generates 100-fold less wear debris than metal-on-polyethylene. *Acta Orthop. Scand.* **1999**, *70*, 578–582. [[CrossRef](#)] [[PubMed](#)]
64. Anissian, H.L.; Stark, A.; Good, V.; Dahlstrand, H.; Clarke, I.C. The wear pattern in metal-on-metal hip prostheses. *J. Biomed. Mater. Res.* **2001**, *58*, 673–678. [[CrossRef](#)] [[PubMed](#)]
65. Clarke, I.C. Science Friction applied to MOM Bearings. In *ASTM workshop on Characterization of Metal-on-Metal (MOM) Hip Replacement Devices*; ASTM: Anaheim, CA, USA, 2011.
66. Halim, T.; Clarke, I.C.; Burgett-Moreno, M.; Donaldson, T.K.; Savisaar, C.; Bowsher, J.G. A Simulator Study of Adverse Wear with Metal and Cement Debris Contamination in metal-on-metal (MOM) Hip Bearings. *J. Bone Jt. Res. UK* **2015**, *4*, 29–37. [[CrossRef](#)] [[PubMed](#)]
67. Clarke, I.C.; Lazennec, J.Y.; Brusson, A.; Savisaar, C.; Bowsher, J.G.; Burgett, M.; Donaldson, T.K. Risk of Impingement and Third-body Abrasion With 28-mm Metal-on-metal Bearings. *Clin. Orthop. Relat. Res.* **2014**, *472*, 497–508. [[CrossRef](#)] [[PubMed](#)]
68. Clarke, I.C.; Manley, M.T. How do alternative bearing surfaces influence wear behavior? *J. Am. Acad. Orthop. Surg.* **2008**, *16*, S86–S93. [[CrossRef](#)] [[PubMed](#)]

69. Halim, T.; Burgett, M.; Donaldson, T.K.; Savisaar, C.; Bowsher, J.G.; Clarke, I.C. Profiling the third-body wear damage produced in CoCr surfaces by bone cement, CoCr, and Ti6A14V debris: A 10-cycle metal-on-metal simulator test. *Proc. Inst. Mech. Eng. H* **2014**, *228*, 703–713. [[CrossRef](#)] [[PubMed](#)]
70. McPherson, E.J.; Clarke, I.C.; Donaldson, T.K.; Burgett, M.D. A MOM dislocator case demonstrating importance of impingement damage in triggering adverse 3rd-body abrasive wear risks. *Orthopedics Today*, 13–16 January 2013.



© 2017 by the authors. Licensee MDPI, Basel, Switzerland. This article is an open access article distributed under the terms and conditions of the Creative Commons Attribution (CC BY) license (<http://creativecommons.org/licenses/by/4.0/>).